Invited Paper

New photonic-crystal system for integrated optics

Steven G. Johnson,* M. L. Povinelli, J. D. Joannopoulos
Department of Physics and Center for Materials Science and Engineering,
Massachusetts Institute of Technology

ABSTRACT

We describe a new photonic-crystal structure with a complete three-dimensional photonic band gap (PBG) and its potential application to integrated optics. The structure not only has a large band gap and is amenable to layer-by-layer litho-fabrication, but also introduces the feature of high-symmetry planar layers resembling two-dimensional photonic crystals. This feature enables integrated optical devices to be constructed by modification of only a single layer, and supports waveguide and resonant-cavity modes that strongly resemble the corresponding modes in the simpler and well-understood 2d systems. In contrast to previous attempts to realize 2d crystals in 3d via finite-height "slabs," however, the complete PBG of the new system eliminates the possibility of radiation losses. Thus, it provides a robust infrastructure within which to embed complex optical networks, combining elements such as compact filters, channel-drops, and waveguide bends/junctions that have previously been proposed in 2d photonic crystals.

Keywords: photonic crystal, photonic band gap, waveguide, resonant cavity, integrated optics

1. INTRODUCTION

Much research in recent years has been focused on photonic crystals: periodic dielectric (or metallic) structures with a photonic band gap (PBG), a range of frequencies in which light is forbidden to propagate.[1,2] Photonic crystals provide an unprecedented degree of control over light, introducing the possibility of many novel optical devices and effects.[3] One important area for potential applications is that of integrated optics; here, the band gap allows miniaturization to the ultimate wavelength scale while eliminating the inefficiencies and complexites caused by radiation losses in such devices. Generally speaking, there have been two main categories of study regarding photonic-crystal systems for integrated optics: first, analyzing the phenomena and potential devices that a PBG makes possible; and second, figuring out how to realize these effects in practice. In this paper, we bridge the gap between these two categories—we describe a new three-dimensional crystal, amenable to layer-by-layer lithographic fabrication, that permits the direct realization of theoretical results from two dimensions.[4,5]

1.1 Photonic-crystal theory and devices in two dimensions

In order to understand PBG phenomena and to propose useful optical components that photonic crystals might make possible, researchers have often focused on two-dimensional systems. Working in two dimensions has many advantages, in addition to the substantial computational savings versus 3d. The electromagnetic fields are completely TE or TM polarized, with the electric or magnetic field, respectively, entirely in the plane—this reduces the vectorial Maxwell's equations to a *scalar* problem in terms of the field (magnetic or electric, respectively) perpendicular to the plane. As a result of this scalar, two-dimensional nature, visualization and understanding of theory and simulation are greatly simplified. Band gaps are achieved with uncomplicated structures, and symmetries are obvious. We could continue *ad nauseam*, but let us mention one last attraction of two dimensions that is particularly relevant in device design: when trapping light in linear defects (waveguides) and point defects (microcavities), the fixed polarization and simple geometries make it easy to predict, analyze, and manipulate the character of the localized modes introduced by the defects.

In two dimensions, photonic band gaps have been shown to make possible a number of useful optical components, some of which are depicted in Figure 1: sharp bends,[6] efficient waveguide splitters[7] and intersections,[8] and channel-dropping filters.[9,10] All of these devices are designed by combining a few well-understood elements (waveguides and cavities) and by employing general principles of resonance, symmetry, and coupled-mode theory. The attainable device characteristics are thereby known *a priori*, and minimal tuning is required to push the precise numerical results to the desired values. What makes all of this possible is the photonic band gap: it forces the light to exist only in one of a few states or channels, and transforms a problem with infinitely many directions of propagation into a one-dimensional system with a small number of variables. Although the same ideas can be then applied to conventional waveguides employing total internal reflection,[11,12] the inevitable

* stevenj@alum.mit.edu; phone 617-253-4780; fax 617-253-2562; http://ab-initio.mit.edu/

Active and Passive Optical Components for WDM Communication, Achyut K. Dutta,
Abdul Ahad S. Awwal, Niloy K. Dutta, Katsunari Okamoto, Editors, Proceedings of SPIE
Vol. 4532 (2001) © 2001 SPIE · 0277-786X/01/$15.00

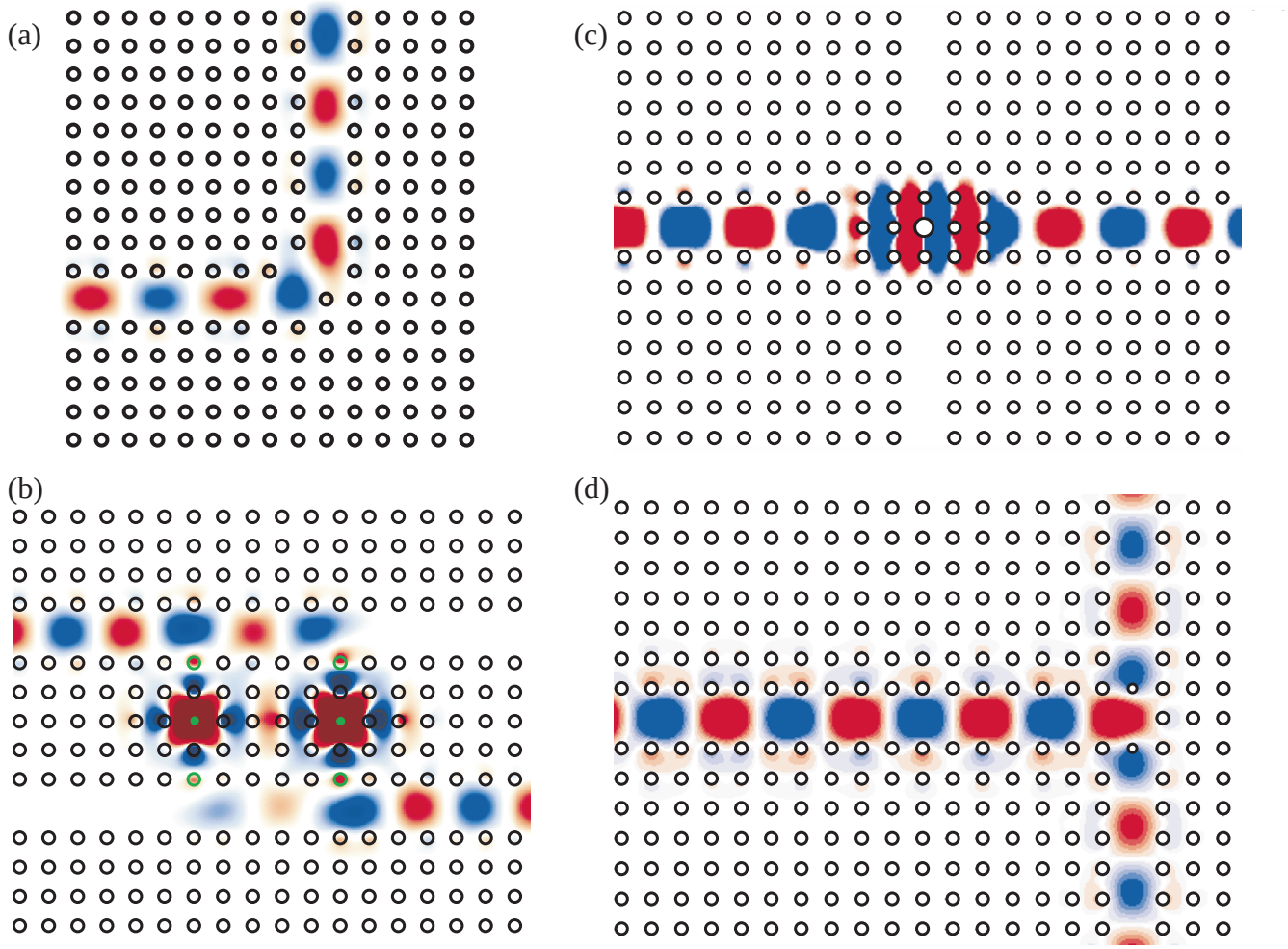

Figure 1: Photonic-crystal devices in a two-dimensional crystal (square lattice of dielectric rods in air), showing the TM electric field value (red/blue = positive/negative) with ε contours in black. All four devices have essentially 100% transmission, with no reflections or losses. (a) 90° waveguide bend. (b) Channel-dropping filter. (c) Intersection of two waveguides without crosstalk. (d) Waveguide splitter/junction.

radiation losses of those systems spoil the perfection of the theory (and the devices)—such losses generally require *ad hoc* tuning to minimize, and greatly complicate the design, usage, and understanding of any component.

For example, consider the case of the waveguide bend in Figure 1(a). Because of the photonic band gap, light can do only one of two things when it hits the bend: go forward, or go back. The radiation that would plague any sharp bend in a conventional waveguide is completely absent, since light cannot propagate in the bulk crystal. Moreover, if the waveguide and bend region support only single-mode propagation, the problem can be described effectively as transmission through a one-dimensional potential well. If the bend/well is symmetric, a well-known result predicts resonant frequencies with 100% transmission, and nearly the exact transmission curve can be calculated via this model.[6] Significantly, these predictions are independent of the exact crystal or waveguide structure, and depend only upon their symmetry and single-modality.

1.2 Photonic-crystal slabs

In order to realize two-dimensional photonic-crystal designs in three dimensions, one would ideally like to use the same 2d pattern for the 3d structure. However, one then encounters an obvious difficulty: how is the light confined in the third dimension? Or indeed, if one takes into account the third dimension, is there any longer a band gap? One possible answer to these questions has come in the form of photonic-crystal slabs, as depicted in Figure 2: two-dimensional photonic-crystal patterns with a finite height, that use index-guiding (a.k.a. total internal reflection) to confine light vertically.[13–18] In this case, the higher index of the slab (compared the the material above and below) produces guided modes confined to the vicinity of the slab, and the periodicity creates a "band gap" where no guided modes exist.[14] Although this is not a complete gap due to the presence of

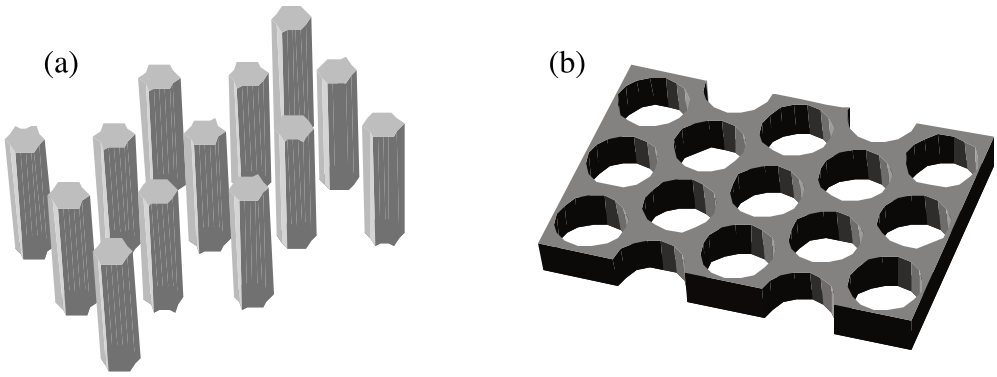

Figure 2: Two typical photonic-crystal slabs, dielectric structures with two-dimensional periodicity and a finite height—they use in-plane photonic band gaps and vertical index-guiding. (a) Triangular lattice of dielectric rods in air. (b) Triangular lattice of air holes in dielectric.

radiating modes at all frequencies (the light cone), it can be used to losslessly confine light in linear waveguides and to imperfectly trap light in resonant cavities.[13,16–18] The lack of a complete band gap leads to a number of difficulties, however. First, whenever translational symmetry is broken (e.g. by a bend or a cavity), radiation losses are inevitable—although such losses can often be minimized,[16–18] they must be continually taken into account, just as for conventional waveguides. A second limitation is that the need for waveguide modes to be index-guided, and thus to lie underneath the light line, produces a limited bandwidth and low group velocities in a periodic slab (compared to two-dimensional crystals or to conventional waveguides); we will demonstrate this below. Nevertheless, because of their relative ease of fabrication, slab structures continue to attract considerable experimental and theoretical attention. Another interesting system with somewhat different tradeoffs uses in-plane resonant modes *above* the light line (i.e. not guided), which more closely model the two-dimensional modes at the expense of large aspect ratios required everywhere to minimize radiation losses.[18]

1.3 Three-dimensional photonic crystals

A full realization of a photonic band gap requires a crystal periodic in all three dimensions, and many such structures have been proposed.[19–30] Some of the most attractive systems for integrated optics are planar-layer structures:[25–29] these have piecewise-constant cross-sections, and can thus be fabricated in a layer-by-layer fashion using traditional micro-lithography. The fine control provided by lithography promises the ability to precisely place defects in the crystal in order to construct integrated optical devices. The planar-layer crystal that has been most commonly fabricated (with success even at micron lengthscales[31–34]), is the "layer-by-layer"[25] (or "woodpile"[26]) structure—dielectric "logs" stacked in alternating perpendicular directions with a 4-layer period, forming an fcc crystal oriented in the 100 direction. However, this and other previous planar-layer structures lack rotational symmetry in any given plane, meaning that integrated optical networks will require defects to extend across multiple layers of the structures. Moreover, the nature of the defect modes so confined will have significant qualitative differences from those in two-dimensional crystals, because the dielectric structure where the mode resides does not resemble a 2d crystal.

1.4 A new three-dimensional crystal

We have proposed[4] a new planar-layer photonic crystal with an omnidirectional band gap, depicted in Figure 3, whose layers have high symmetry and whose cross-sections form well-known two-dimensional photonic crystals. The crystal consists of an fcc lattice (possibly distorted) of air (or low-index) cylinders in dielectric, oriented along the 111 direction. Such a lattice results in a graphite-like[20] system of planar layers of the two types from Figure 2: triangular lattices of air holes in dielectric and dielectric cylinders ("rods") in air. The sculptured appearance of the rods is not important and is simply a by-product of a fabrication method (in Figure 4). These layers are stacked in a repeating, 3-layer sequence (along 111) and should be amenable to planar lithographic techniques as discussed below. The band diagram, in Figure 5(a), has a complete gap of over 21% for Si:air dielectric contrast (ε = 12:1 at 1.55μm), and of over 8% even for Si:SiO_2 contrast (ε = 12:2); the PBG persists down to ε contrasts of 4:1 (2:1 index contrast). (Even larger gaps, of over 26%, can be achieved for Si:air by controlling the rod and hole radii independently, at the expense of extra alignment steps in the fabrication process.) The vertical transmission through roughly one period (three bilayers plus a hole layer) of the structure, shown in Figure 5(b), is attenuated by about 20dB in the gap.

Because of the high-symmetry, 2d-crystal cross sections, most integrated devices will require modification of only a single

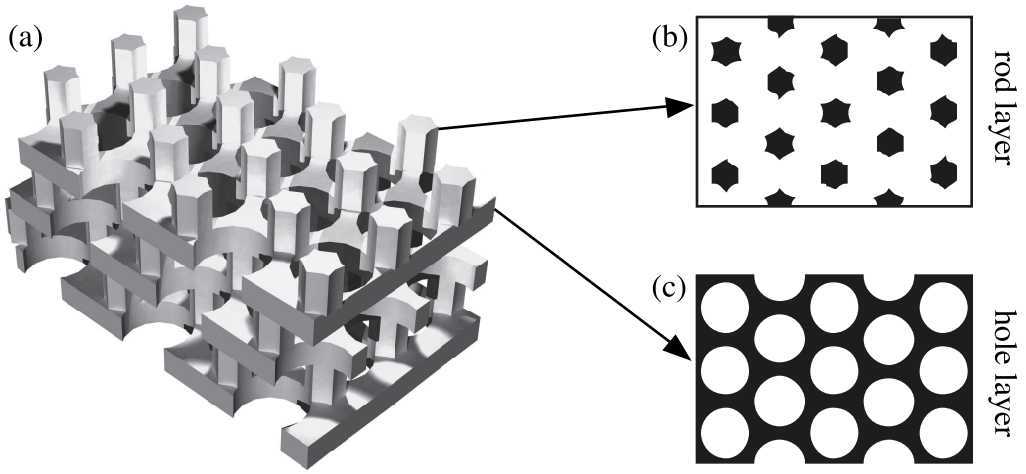

Figure 3: (a) Computer rendering of a novel 3d photonic crystal, showing several horizontal periods and one vertical period, consisting of an fcc lattice of air holes (radius 0.293*a*, height 0.93*a*) in dielectric (21% fill). This structure has a 21% gap for a dielectric constant of 12. The lattice produces an alternating sequence of two layers, whose cross sections are: (b) rod layer and (c) hole layer.

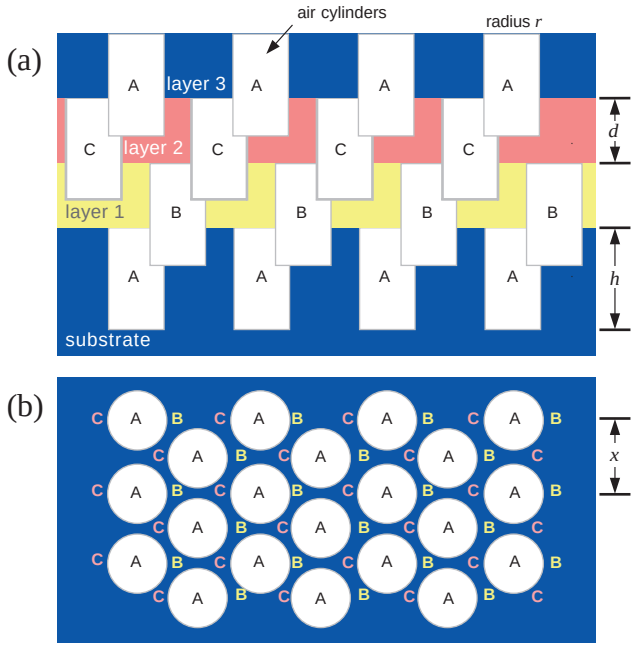

Figure 4: Schematic of the crystal in Figure 3. (a) The vertical structure, showing the different material layers as they might be deposited during fabrication. (The layers are given different colors for clarity, but would normally be the same material and thickness.) (b) Plan view of a horizontal cross section intersecting the "A" cylinders, with the offset locations of cylinders in the other layers also labeled.

layer of the crystal. Moreover, when one forms waveguides, cavities, and other components by introducing defects into the crystal, the resulting optical modes (and thus behaviors) closely resemble those in the corresponding two-dimensional photonic crystal. This should allow designs and results from the simpler 2d systems to be applied almost directly in three dimensions—and, at the same time, the complete band gap totally prohibits radiation losses. Moreover, because the defect modes of the 3d crystal can be visualized and understood largely in terms of their mostly-polarized in-plane cross sections, much of the theoretical simplicity of the original two-dimensional structures is retained. Unlike the 2d systems, where the band gap is typically only for the TM or TE polarization of in-plane light, the band gap in our crystal extends for all possible polarizations and propagation directions of light.

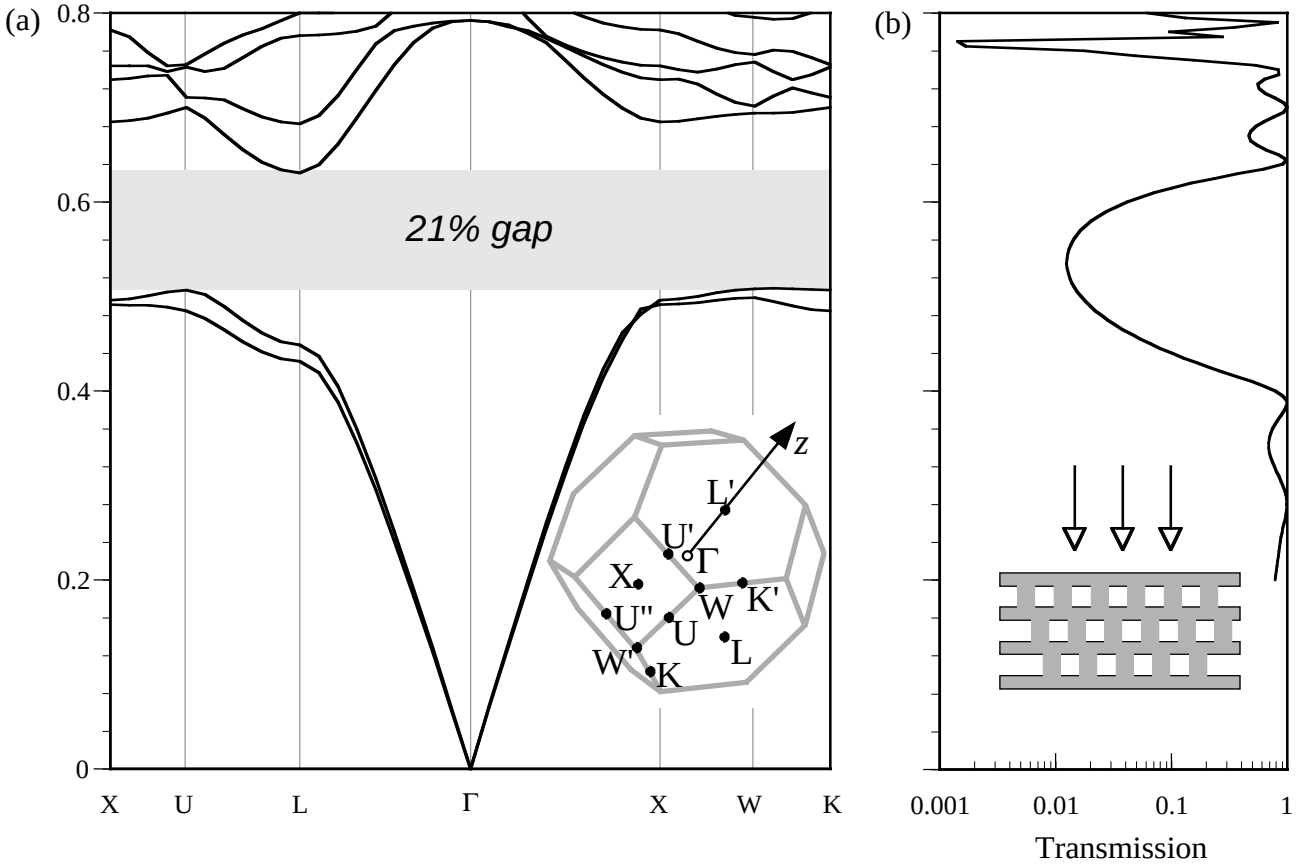

Figure 5: (a) Band diagram for the structure in Figure 3, showing frequency in scale-invariant units vs. wavevector along important symmet directions in the irreducible Brillouin zone. the inset shows the first Brillouin zone and its symmetry points. (b) Vertical transmission spectru for slightly over one period (three layers plus a capping hole layer, as shown in the inset) of this structure, showing the $\Gamma - L'$ gap.

2. COMPUTATIONAL METHODS

Most of the computations in this paper are eigenmode analyses of our photonic crystal and of defect modes therein, yielding the band structures, dispersion relations, and eigen-fields of the perfect crystal, waveguides, and resonant cavities. These fully-vectorial eigenmodes of Maxwell's equations were computed with periodic boundary conditions by preconditioned conjugate-gradient minimization of the block Rayleigh quotient in a planewave basis, using a freely available software package.[36] For waveguides and resonant cavities, the periodic boundary conditions involve a supercell approximation, where the supercell boundaries are placed sufficiently far from the defect so as to not affect the frequency or field of localized modes. (Because of the large band gap, the modes are strongly localized and the supercell size need not be more than a few lattice constants.)

The transmission spectrum of Figure 5(b) is the result of a 3d finite-difference time-domain (FDTD) simulation[37] with a normal-incidence ($\Gamma - L'$) planewave source, absorbing boundaries above and below, and periodic boundaries at the sides.

3. BULK CRYSTAL PARAMETERS AND FABRICATION

The band diagram depicted in Figure 5(a) is for air holes of radius r=0.293a and height h=0.93a (a is the fcc lattice constant) and a dielectric constant ε=12, and has a 20.9% complete PBG. (There are other symmetry points in the irreducible Brillouin zone of this structure that were calculated but are not shown in the band diagram, because their band edges do not determine the gap in this case.) These are the parameters that we use for the bulk crystal in the subsequent defect computations.

More generally, one can apply a trigonal distortion to the fcc lattice of our structure to obtain a trigonal lattice without breaking any additional symmetry. The lattice vectors in this case become the three permutations of $(1, 1, z)a/2$ ($z = 0$ for

fcc), with layer-thickness $d = |1 + z/2|a/\sqrt{3}$ and in-plane lattice constant $\bar{a} = |1 - z|a/\sqrt{2}$ as defined in Figure 4. The parameter z can be varied to further optimize the gap. The parameters of Figure 3 were optimal for the fcc case of $z = 0$; we also maximized the gap for varying z and dielectric contrast, with results in Table I. In general, the structure strongly prefers the fcc case with its nearly-spherical Brillouin zone, and distortions seem to increase the gap percentage by no more than 0.5.

Table I. Optimal parameters and gaps for various dielectric contrasts.

ε contrast	r	h	z	mid-gap ν	gap size
12:1 (Si:air)	0.285a	0.960a	0.0165	0.579 c/a	21.4%
6:1 12:2 (Si:SiO_2)	0.273a	0.908a	–0.00246	0.648 c/a 0.458 c/a	8.4%
4.5:1	0.265a	0.900a	–0.00612	0.688 c/a	2.7%
4:1 (SiO_2:air)	0.259a	0.895a	–0.00778	0.699 c/a	0.33%

Our photonic-crystal is amenable to layer-by-layer fabrication, which might proceed along the following schematic lines, as depicted in Figure 4. First, a layer of cylindrical holes (labelled "A") are etched into a high-index substrate (e.g. Si). Next, the holes are back-filled with another material (e.g. SiO_2), the surface is planarized to the top of the high-index substrate, and a second layer of high-index material ("layer 1") is grown on top. Then, the next layer of holes ("B") is etched to the appropriate depth, but offset from the "A" holes as shown in the Figure 4(b). This back-filling, planarizing, growth, and etching is repeated for the "C" holes and then for the next layer of "A" (in "layer 3"), at which point the structure repeats itself. When the desired layers are grown, the back-fill material is removed (e.g., by a solvent), and a high-contrast photonic-crystal is obtained. A similar process has been successfully employed for the "layer-by-layer" structure, testifying to the feasibility of this method.[31,32] Other variations are possible. One could leave the backfill material in the structure if it is low-index, and a complete PBG (albeit smaller, 8.4% for Si/SiO_2) can still be obtained; equivalently, a lower-index substrate could be used with air holes. Also, the layers could be fabricated individually, and then inverted and bonded together; this method has likewise been proven on the layer-by-layer structure.[33,34] Alternatively, one may fabricate the rod and hole layers using separate steps, requiring twice as many interlayer alignments but removing the need to etch two materials simultaneously. (A very similar structure was thus fabricated for 8μm wavelength, although the existence of a gap was not determined.[35]) Our calculations show that the resulting extra degree of freedom, the rod radius, allows a maximum gap of over 26% for Si/air.

We have studied the confinement of light in waveguides and resonant cavities created by making defects in a single layer of the bulk crystal, either a rod layer or a hole layer, and we discuss these results in the following sections.[5] We show that the corresponding localized modes correspond precisely to those supported in the analogous two-dimensional crystal and defect. For these calculations, we use the parameters r=0.293a, h=0.93a, z=0 (fcc), and ε=12. In order to facilitate comparison to the two-dimensional structures, we switch to units of $\bar{a}$ (the in-plane lattice constant) for distance, $2\pi/\bar{a}$ for wavevectors, and $c/\bar{a}$ for frequency. In these units, the hole radius is $r_h = 0.414\bar{a}$, and the thickness of a hole layer is $0.318\bar{a}$. The radius of a cylindrical rod with the same area as a rod in the structure is $r_r = 0.175\bar{a}$, and the thickness of a rod layer is $0.500\bar{a}$.

4. LINEAR DEFECTS: WAVEGUIDES

By creating a linear defect in a photonic crystal, a waveguide may be formed.[3] By adding or removing dielectric, one or more states are pulled down or pushed up into the gap, respectively, and are thereby localized to the vicinity of the defect. Since discrete translational symmetry remains in the direction parallel to the waveguide, the wavevector in this direction is conserved—the states propagate without scattering, and their frequencies can be plotted versus wavevector to form a continuous dispersion relation. Because our crystal has a complete band gap, the modes decay exponentially away from the waveguide in all directions, including vertically, so the mode is strongly confined to the planar layer of the defect—for this reason, we can hope that the modes will strongly resemble those in the corresponding two-dimensional structure, and this hope is justified numerically below.

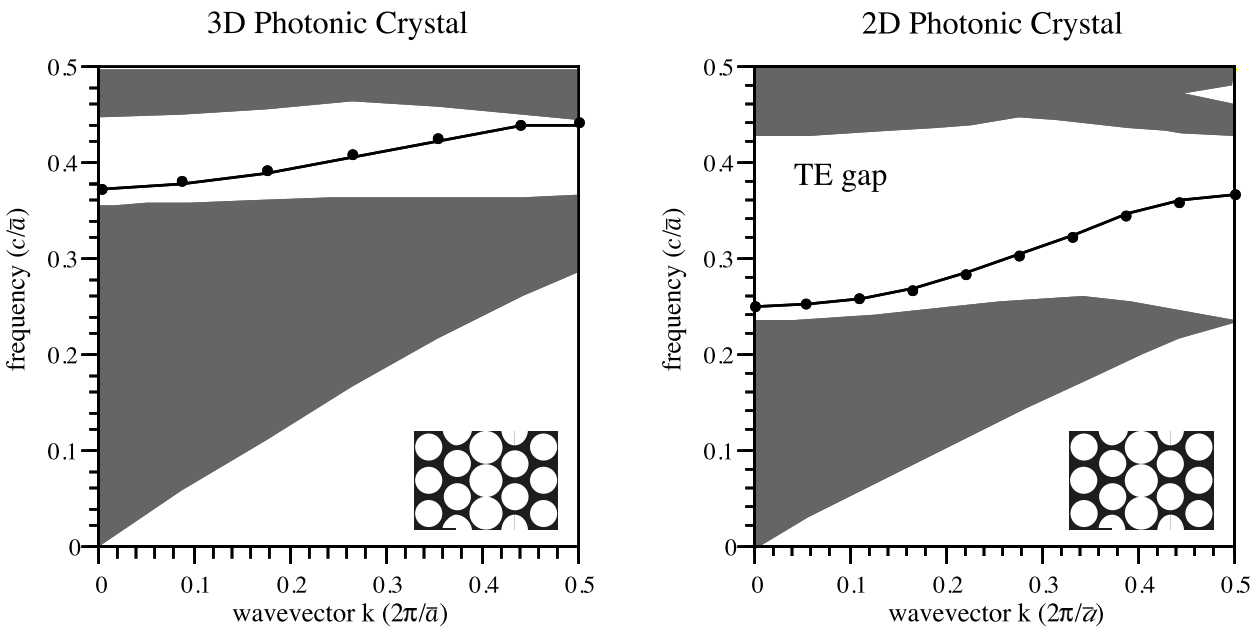

Figure 6: (a) Projected band structure for the 3d crystal with a linear defect created by altering a single hole layer. Shown in the inset is a horizontal cross section through the mid-plane of the defect. The defect holes have radius $r_h' = 0.5\bar{a}$, vs. $r_h = 0.414\bar{a}$ in the bulk, where $\bar{a}$ is the in-plane lattice constant. (b) Projected band structure for the TE modes of the 2d crystal with identical geometry to the cross-section of the 3d crystal shown in (a).

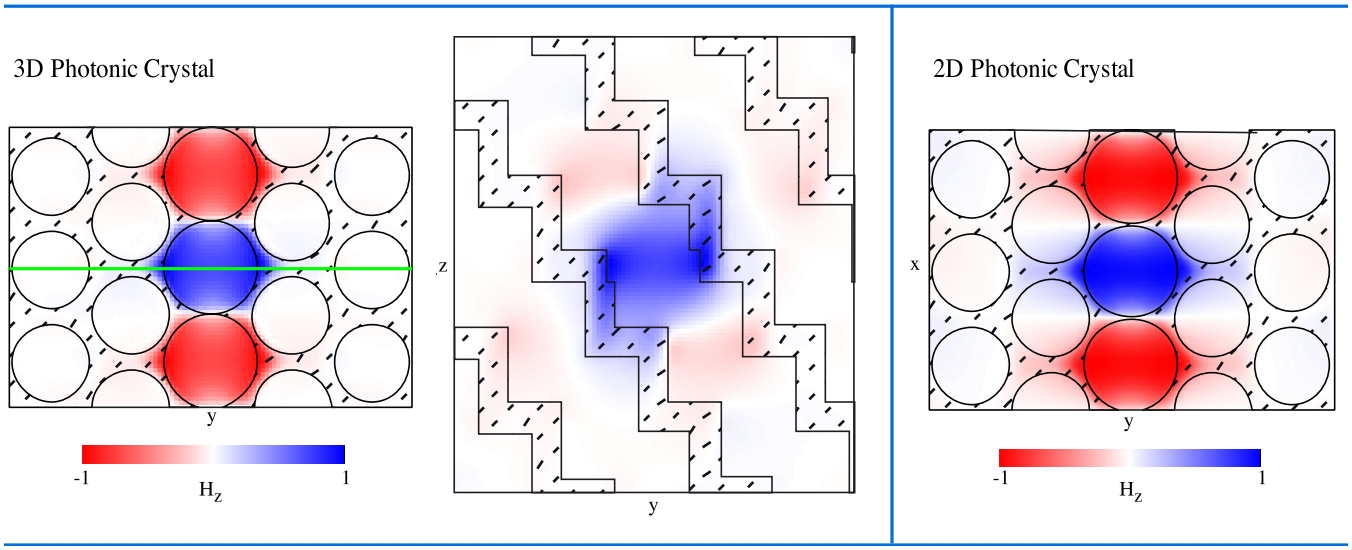

Figure 7: Mode profiles for the increased-hole linear-defect states from Figure 6 at the Brillouin zone edge. Overlaid cross hatches indicate regions of high dielectric material. (a–b) The field for the 3d linear-defect structure corresponding to Figure 6(a). H_z is plotted for horizontal and vertical cross sections of the 3d crystal. The cross sections intersect along the green lines on the figures. (c) H_z for the 2d linear-defect structure from Figure 6(b).

4.1 A waveguide in the hole layer

We first consider waveguides formed by modifying a *single hole layer* of the 3d photonic crystal, increasing the radii of a line of nearest-neighbor holes from $r_h = 0.414\bar{a}$ to $r_h' = 0.5\bar{a}$ (tangent). We will show that this introduces a TE-like mode into the hole layer, just as the corresponding two-dimensional structure (with a TE band gap) supports a TE guided mode. The

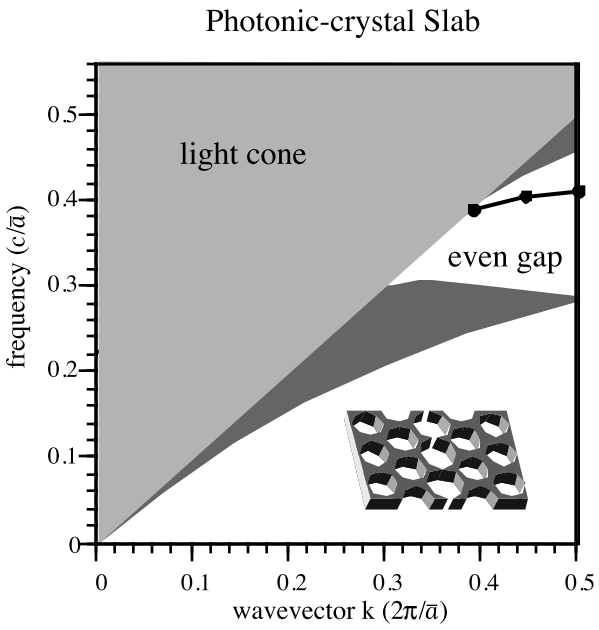

Figure 8: Projected band structure for a photonic-crystal slab, with a linear defect as in Figure 6. A rendering of the slab and defect is shown in the inset; its thickness is $0.71\bar{a}$. The light-grey region indicates the light cone; dark-grey regions indicate even-symmetry (TE-like) modes of the bulk structure. The solid-dot line is the guided mode in the defect region, similar to those of Figure 7.

dispersion relation for the 3d line-defect structure is shown in Figure 6(a) and compared with that for the 2d structure (with the same cross-section) in Figure 6(b). Shaded regions indicate extended states in the perfect crystal, and for the 2d structure only TE modes are shown. In both cases, we observe that the waveguide is single-mode: a single defect band extends almost all the way across the gap, but does not intersect the band edges.

In addition to the resemblance in band structures, there is a strong, quantifiable similarity between the defect modes in the 3d and 2d crystals. Figure 7(a–b) shows the magnetic-field z-component for the 3d defect state at the $k = \pi/\bar{a}$ edge of the Brillouin zone, with horizontal and vertical cross-sections bisecting the hole layer, along with its 2d counterpart in Figure 7(c). The fields exhibit a clear visual similarity, indicating the analogous character of the defect modes in 2d and 3d, and this similarity can be quantified in two ways. First, just as the 2d state is purely TE, the 3d field is 98% TE polarized in the horizontal mid-plane of the layer, defined by:

$$R_H = \frac{\int |H_z(\vec{r})|^2 dxdy}{\sum_j \int |H_j(\vec{r})|^2 dxdy} \approx 0.98 . \quad (1)$$

Second, the overlap integral between the 2d and 3d field profiles in the mid-plane is found to be 94%, defined by:

$$O_H = \left| \frac{\int \vec{H}^{3D}(\vec{r})^* \cdot \vec{H}^{2D}(\vec{r}) dxdy}{\sqrt{(\int |\vec{H}^{3D}(\vec{r})|^2 dxdy)\int |\vec{H}^{2D}(\vec{r})|^2 dxdy}} \right|^2 \approx 0.94 . \quad (2)$$

For comparison, we consider the analogous waveguide in a photonic-crystal slab. Here, the photonic-crystal slab has the same cross-section as that of a hole layer, but is surrounded by air and has a thickness of $0.71\bar{a}$ (chosen to approximately maximize its gap[14]). In Figure 8, we exhibit the dispersion relation for an equivalent hole-defect waveguide in the photonic-crystal slab, and the differences with those of Figure 6 are striking. The slab band diagram is shadowed by a light cone (the light-grey region); only those modes lying beneath the light cone are vertically confined by index-guiding. Thus, the slab waveguide mode only exists near the edge of the Brillouin zone where its group velocity goes to zero, and consequently it has a narrow bandwidth.

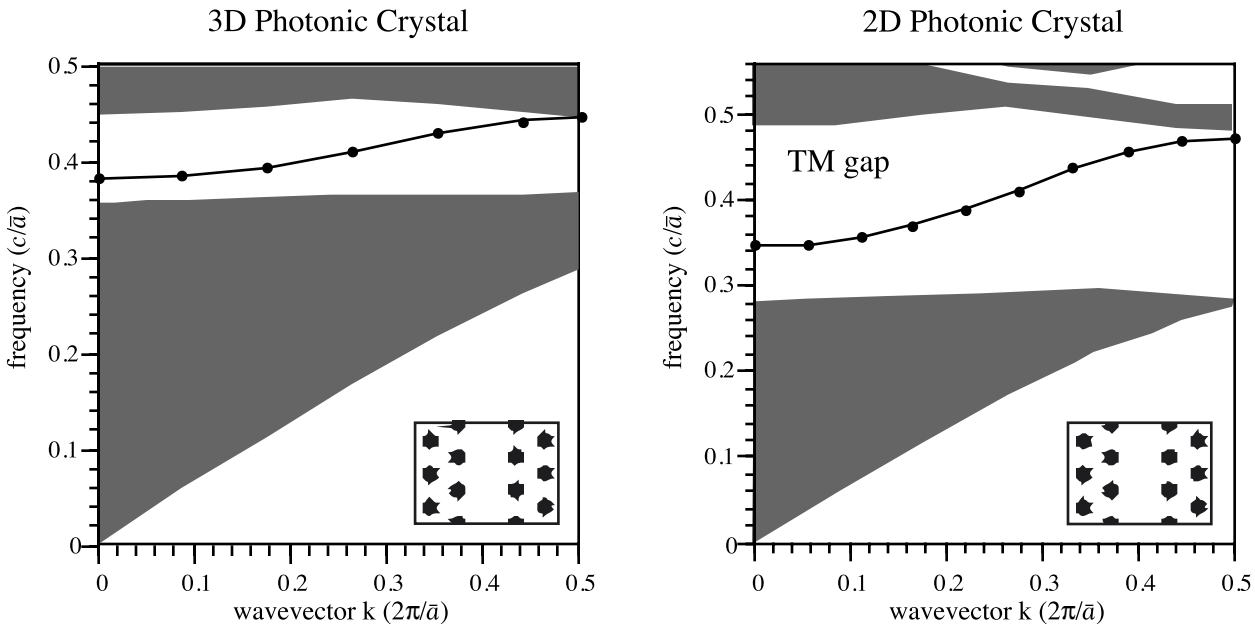

Figure 9: (a) Projected band structure for the 3d crystal with a linear defect created by removing a row of nearest-neighbor rods in a single rod layer, resulting in the cross section shown in the inset. (b) Projected band structure for the TM modes of the corresponding 2d crystal.

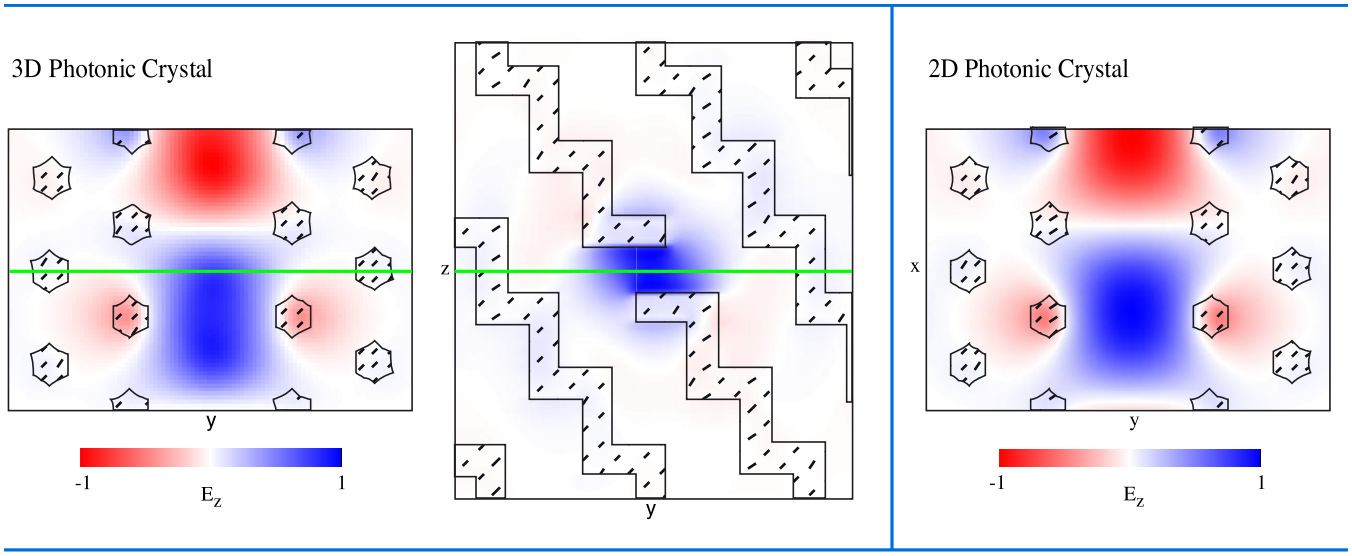

Figure 10: Mode profiles for the removed-rod linear-defect state of Figure 9 at $k = 0.53\pi/\bar{a}$. (a–b) Field for the 3d linear-defect structure of Figure 9(a), with E_z plotted for horizontal and vertical cross-sections. (c) Field for the 2d structure of Figure 9(b).

4.2 A waveguide in the rod layer

We have shown that a TE-like defect mode can be introduced into the 3d photonic crystal by altering a hole layer. A TM-like defect mode can similarly be created by modifying a rod layer of the structure. In this case, we completely remove a row of nearest-neighbor rods to form the defect, relying upon the dramatic ability of a photonic crystal to guide light even in air. Again, we compare to the analogous defect in a 2d crystal, this time a rod lattice (with a gap in its TM modes). The resulting dispersion relations in Figure 9, as before, display in both cases a single-mode band that covers almost the entire gap and extends over the entire Brillouin zone.

The field profiles, this time for the *z*-component of the electric field (due to the TM polarization) at $k = 0.53\pi/\bar{a}$, are shown in Figure 10. Almost indistinguishable to the eye, they testify to the close physical connection between the behaviors of

the two systems. Just as for the hole-layer waveguide, we quantify this similarity in two ways. First, just as the 2d mode is purely TM, the 3d mode is 99% TM-polarized in the mid-plane, defined by:

$$R_E = \frac{\int |E_z(\vec{r})|^2 dxdy}{\sum_j \int |E_j(\vec{r})|^2 dxdy} \approx 0.99 . \quad (3)$$

Second, the overlap integral between the 2d and 3d field profiles in the mid-plane is 98%, defined by a slightly different expression than Eq. (2) because of the peculiar orthonormality metric of the electric field:

$$O_E = \left| \frac{\int \varepsilon(\vec{r}) \vec{E}^{3D}(\vec{r})^* \cdot \vec{E}^{2D}(\vec{r}) dxdy}{\sqrt{\int \varepsilon(\vec{r}) |\vec{E}^{3D}(\vec{r})|^2 dxdy \int \varepsilon(\vec{r}) |\vec{E}^{2D}(\vec{r})|^2 dxdy}} \right|^2 \approx 0.98 . \quad (4)$$

If we instead consider a photonic-crystal slab with the cross-section of the rod layer and a thickness of $2\bar{a}$ to approximately maximize its gap, we find that there is no guided mode at all (or, at best, one very weakly guided at the upper edge of the gap). This is, indeed, the expected result—by removing a row of rods from a slab, there is no longer enough index contrast to guide the mode in the vertical direction.[15] In other words, the guided bands of Figure 9 lie inside the light cone of an index-guided slab.

5. POINT DEFECTS: RESONANT CAVITIES

Next to waveguides, the other major building block for optical devices is the resonant cavity, which traps one or more discrete electromagnetic modes in a point-like region (confined in all three dimensions). They are "resonant" modes because they do leak out eventually—this is by design, since the light has to escape in order to be useful. The light must only escape, however, into specific desired channels, typically into a waveguide, and therein lies the problem with resonant cavities in conventional systems (e.g. ring resonators) and photonic-crystal slabs. In the absence of a complete photonic band gap, losses from the cavity into the radiation continuum are inevitable, and minimization of these losses requires tradeoffs such as delocalization[16,18] or careful tuning.[17] In contrast, with a 3d photonic crystal, radiation leakage can be made arbitrarily small merely by adding more layers of bulk crystal around the cavity—like the two-dimensional devices of Figure 1, the cavity can only decay into deliberately introduced channels. Microcavities are created by introducing a localized defect into the 3d crystal, and can be designed to have any desired symmetry and frequency. In this section, we create such point defects by modifying only a single hole or rod layer of the crystal, and demonstrate how we can mimic the behavior of the analogous 2d crystal defect.

We first create a cavity in a hole layer, by increasing the radius of a single hole to $r_h' = 0.5\bar{a}$. This creates a single TE-like defect mode in the gap (0.36–0.44$c/\bar{a}$) at a frequency of $0.40c/\bar{a}$. Horizontal and vertical cross sections of the magnetic-field *z*-component are shown in Figure 11, along with those of the corresponding 2d defect mode. (The 2d defect mode has a frequency of $0.28c/\bar{a}$, in the TE gap from 0.26–0.43$c/\bar{a}$.) As was seen with the waveguide modes, the field patterns are almost identical in 3d, with $R_H \approx 0.98$ (98% TE) and an overlap of $O_H \approx 0.92$.

Likewise, a cavity is created in a rod layer by removing a single rod, producing a single TM-like defect mode in the gap at a frequency of $0.41c/\bar{a}$. The corresponding 2d structure, with a TM gap from 0.30–0.48$c/\bar{a}$, has a defect mode at $0.41c/\bar{a}$. Horizontal and vertical cross sections of the electric-field *z*-component are shown in Figure 12 for both the 3d and 2d modes. Again, the similarity in field patterns can be quantified by the polarization $R_E \approx 0.99$ (99% TM) and an overlap of $O_E \approx 0.97$.

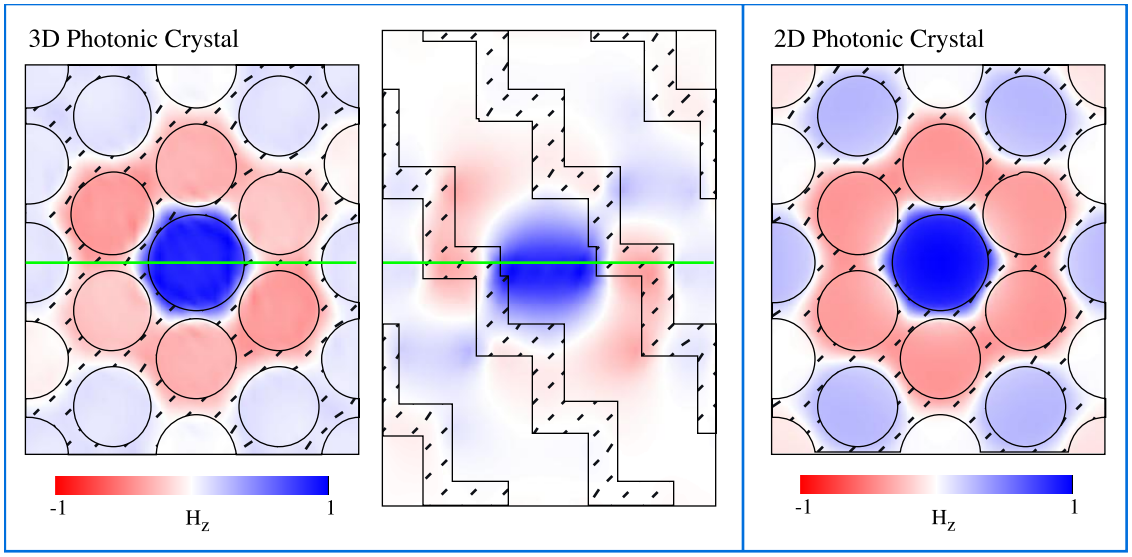

Figure 11: (a–b) Mode profile for a point defect in the 3d crystal, created by increasing the radius of a single hole to $r_h' = 0.5\bar{a}$ in one hole layer. H_z is plotted for horizontal and vertical cross sections. (c) Mode profile for the TE defect state in the corresponding 2d crystal.

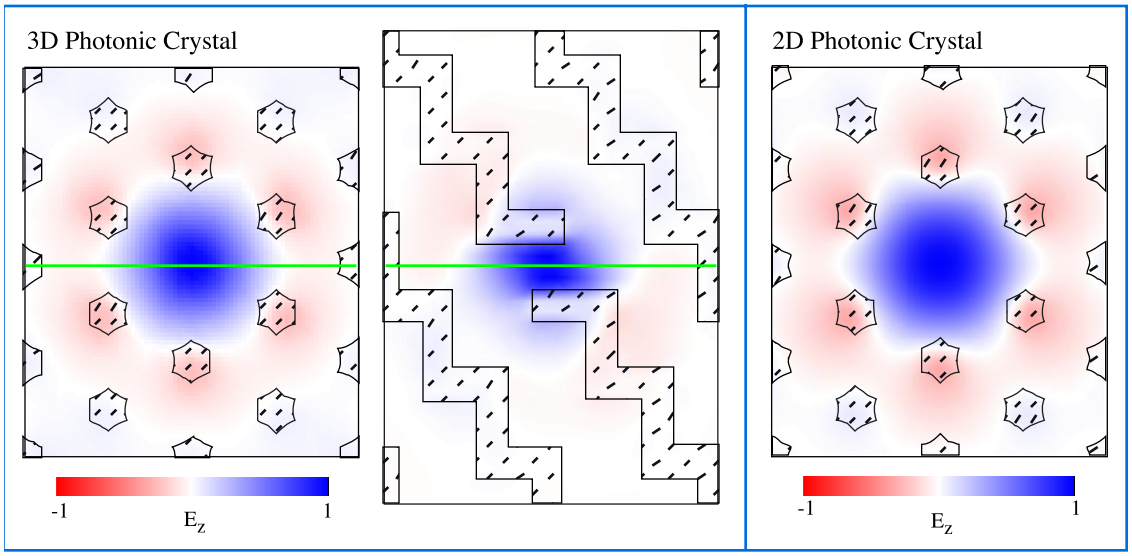

Figure 12: (a–b) Mode profile for a point defect in the 3d crystal, created by removing a single rod from one rod layer. E_z is plotted for horizontal and vertical cross sections. (c) Mode profile for the TM defect state in the corresponding 2d crystal.

6. CONCLUSION

In summary, we have demonstrated a photonic-crystal structure with a complete three-dimensional band gap. This structure has a very large gap, is tolerant of low index contrast, is amenable to layer-by-layer fabrication, and can be thought of as a stack of 2d photonic-crystal layers. This last feature, in the context of a large three-dimensional gap, permits simplified construction of complicated optical networks by modifying only a single layer, without breaking symmetry between different directions in the plane. We have shown how the defect modes thus created are almost identical to those in the corresponding two-dimensional system. This allows one to build on the many theoretical and computational attractions of 2d, as well as the large body of existing work and analyses for those basic systems, without the inherent problems of losses due to the lack of a complete PBG. Moreover, because of the similarity in the defect states and the complete band gap, we expect that the behavior of more complicated, integrated devices in this crystal will also quantitatively resemble their two-dimensional counterparts.

ACKNOWLEDGEMENTS

This work was supported in part by the Materials Research Science and Engineering Center program of the National Science Foundation under award DMR-9400334.

REFERENCES

1. E. Yablonovitch, "Inhibited spontaneous emission in solid-state physics and electronics," *Phys. Rev. Lett.* **58**, pp. 2059–2062, 1987.

2. S. John, "Strong localization of photons in certain disordered dielectric superlattices," *Phys. Rev. Lett.* **58**, pp. 2486–2489, 1987.

3. See, *e.g.*, J. D. Joannopoulos, P. R. Villeneuve, and S. Fan, "Photonic crystals: Putting a new twist on light," *Nature* **386**, pp. 143–149, 1997.

4. S. G. Johnson and J. D. Joannopoulos, "Three-dimensionally periodic dielectric layered structure with omnidirectional photonic band gap," *Appl. Phys. Lett.* **77**, pp. 3490–3492, 2000.

5. M. L. Povinelli, S. G. Johnson, and J. D. Joannopoulos, "2D-like defect modes in a 3D photonic crystal," *Phys. Rev. B*, in press, 2001.

6. A. Mekis, J. C. Chen, I. Kurland, S. Fan, P. R. Villeneuve, and J. D. Joannopoulos, "High transmission through sharp bends in photonic crystal waveguides," *Phys. Rev. Lett.* **77**, pp. 3787–3790, 1996.

7. S. Fan, S. G. Johnson, J. D. Joannopoulos, C. Manolatou, and H. A. Haus, "Waveguide branches in photonic crystals," *J. Opt. Soc. Am. B* **18**, pp. 162–165, 2001.

8. S. G. Johnson, C. Manolatou, S. Fan, P. R. Villeneuve, J. D. Joannopoulos, and H. A. Haus, "Elimination of cross talk in waveguide intersections," *Opt. Lett.* **23**, pp. 1855–1857, 1998.

9. S. Fan, P. R. Villeneuve, J. D. Joannopoulos, and H. A. Haus, "Channel drop tunneling through localized states," *Phys. Rev. Lett.* **80**, pp. 960–963, 1998.

10. S. Fan, P. R. Villeneuve, J. D. Joannopoulos, M. J. Khan, C. Manolatau, H. A. Haus, "Theoretical analysis of channel drop tunneling processes," *Phys. Rev. B* **59**, pp. 15882–15892, 1999.

11. C. Manolatou, S. G. Johnson, S. Fan, P. R. Villeneuve, H. A. Haus, and J. D. Joannopoulos, "High-density integrated optics," *J. Lightwave Tech.* **17**, pp. 1682–1692, 1999.

12. C. Manolatou, M. J. Khan, S. Fan, P. R. Villeneuve, H. A. Haus, and J. D. Joannopoulos, "Coupling of modes analysis of resonant channel add-drop filters," *IEEE J. Quantum Electron.* **35**, pp. 1322–1331, 1999.

13. For recent work, see, *e.g.*, *Photonic Crystals and Light Localization*, edited by C. M. Soukoulis, Proceedings of the NATO ASI on Photonic Band Gap Materials, Limin Hersonissou, Crete, Greece, 19–30 June 2000 (Kluwer Academic, Dordrecht, 2001).

14. S. G. Johnson, S. Fan, P. R. Villeneuve, J. D. Joannopoulos, L. A. Kolodziejski, "Guided modes in photonic crystal slabs," *Phys. Rev. B* **60**, pp. 5751–5758, 1999.

15. S. G. Johnson, P. R. Villeneuve, S. Fan, and J. D. Joannopoulos, "Linear waveguides in photonic-crystal slabs," *Phys. Rev. B* **62**, pp. 8212–8222, 2000.

16. P. R. Villeneuve, S. Fan, S. G. Johnson, and J. D. Joannopoulos, "Three-dimensional photon confinement in photonic crystals of low-dimensional periodicity," *IEE Proc. Optoelec.* **145**, pp. 384–389, 1998.

17. S. G. Johnson, S. Fan, A. Mekis, and J. D. Joannopoulos, "Multipole-cancellation mechanism for high-*Q* cavities in the absence of a complete photonic band gap," *Appl. Phys. Lett.* **78**, pp. 3388–3390, 2001.

18. H. Benisty, D. Labilloy, C. Weisbuch, C. J. M. Smith, T. F. Krauss, D. Cassagne, A. Beraud, and C. Jouanin, "Radiation losses of waveguide-based two-dimensional photonic crystals: positive role of the substrate," *Appl. Phys. Lett.* **76**, pp. 532, 2000.

19. K. M. Ho, C. T. Chan, C. M. Soukoulis, "Existence of a photonic gap in periodic dielectric structures," *Phys. Rev. Lett.* **65**, pp. 3152–3155, 1990.

20. C. T. Chan, S. Datta, K. M. Ho, and C. M. Soukoulis, "*A7* structure: A family of photonic crystals," *Phys. Rev. B* **50**, pp. 1988–1991, 1994.

21. B. T. Holland, C. F. Blanford, A. Stein, "Synthesis of macroporous minerals with highly ordered three-dimensional arrays of spheroidal voids," *Science* **281**, p. 538, 1998.

22. J. E. G. J. Wijnhoven, W. L. Vos, "Preparation of photonic crystals made of air spheres in titania," *Science* **281**, p. 802, 1998.

23. K. Busch and S. John, "Photonic band gap formation in certain self-organizing systems," *Phys. Rev. E* **58**, pp. 3896–3908, 1998.

24. E. Yablonovitch, T. J. Gmitter, and K. M. Leung, "Photonic band structure: The face-centered cubic case employing nonspherical atoms," *Phys. Rev. Lett.* **67**, pp. 2295–2298 (1991).

25. K. Ho, C. Chan, C. Soukoulis, R. Biswas, and M. Sigalas, "Photonic band gaps in three dimensions: New layer-by-layer periodic structures," *Solid State Comm.* **89**, p. 413, 1994.

26. H. S. Sözüer and J. P. Dowling, "Photonic band calculations for woodpile structures," *J. Mod. Opt.* **41**, p. 231, 1994.

27. K. M. Leung, "Diamondlike photonic band-gap crystal with a sizable band gap," *Phys. Rev. B* **56**, pp. 3517–3519, 1997.

28. S. Fan, P. R. Villeneuve, R. Meade, and J. D. Joannopoulos, "Design of three-dimensional photonic crystals at submicron lengthscales," *Appl. Phys. Lett.* **65**, pp. 1466–1468 (1994).

29. H. S. Sözüer and J. W. Haus, "Photonic bands: the simple cubic lattice," *J. Opt. Soc. Am. B* **10**, p. 296, 1993.

30. O. Toader and S. John, "Proposed square spiral microfabrication architecture for large three-dimensional photonic band gap crystals," *Science* **292**, pp. 1133–1135, 2001.

31. E. Ozbay, A. Abeyta, G. Tuttle, M. Tringides, R. Biswas, C. T. Chan, C. M. Soukoulis, and K. M. Ho, "Measurement of a three-dimensional photonic band gap in a crystal structure made of dielectric rods," *Phys. Rev. B* **50**, p. 1945 (1994).

32. S. Y. Lin, J. G. Fleming, D. L. Hetherington, B. K. Smith, R. Biswas, K. M. Ho, M. M. Sigalas, W. Zubrzycki, S. R. Kurtz, J. Bur, "A three-dimensional photonic crystal operating at infrared wavelengths," *Nature* **394**, p. 251, 1998.

33. S. Noda, N. Yamamoto, and A. Sasaki, "New realization method for three-dimensional photonic crystal in optical wavelength region," *Jpn. J. Appl. Phys.* **35**, p. L909, 1996.

34. S. Noda, K. Tomoda, N. Yamamoto, A. Chutinan, "Full three-dimensional photonic bandgap crystals at near-infrared wavelengths," *Science* **289**, pp. 604–606, 2000.

35. J. G. Fleming and S. Y. Lin, private communication.

36. S. G. Johnson and J. D. Joannopoulos, "Block-iterative frequency-domain methods for Maxwell's equations in a plane-wave basis," *Opt. Express* **8** (3), pp. 173–190, 2001.

37. See, *e.g.*, K. S. Kunz and R. J. Luebbers, *The Finite-Difference Time-Domain Methods* (CRC, Boca Raton, FL, 1993).